Progress in modeling the chemical bonding in tetrahedral amorphous carbon

J. K. Walters
Department of Physics and Astronomy, University College London, Gower Street, London WC1E 6BT, United Kingdom

K. W. R. Gilkes
School of Physics, University of East Anglia, Norwich NR4 7TJ, United Kingdom

J. D. Wicks
Department of Materials, Oxford University, Parks Road, Oxford OX1 3PH, United Kingdom

R. J. Newport
School of Physical Sciences, The University, Canterbury, Kent CT2 7NR, United Kingdom
(Received 4 March 1998)

The application of the reverse Monte Carlo method to modeling a covalently bonded amorphous material has been investigated, with the aim of generating a physically acceptable model for tetrahedral amorphous carbon (*ta*-C). Four different models, each containing approximately 3000 atoms, have been produced by fitting to experimental neutron diffraction data and by applying various constraints consistent with prior chemical and physical knowledge of the material. Particular attention has been paid to the development of coordination constraints that are a realistic representation of the local bonding environments in the material. A sufficiently large model (with realistic chemical bonding) has been produced for reliable comparison with experimental diffraction data and determination of medium-long range structural characteristics, e.g., clustering. The results show that better agreement with the experimental data is achieved if the model is allowed to include three- and four-membered rings, and that atoms with sp^2 bonds tend to form small clusters and polymerlike chains interlinking regions of sp^3 or "diamondlike" bonding. The inclusion of 5 at. % hydrogen results in a homogeneous distribution of H atoms throughout the network; no preferential bonding to a particular C atom site is revealed. [S0163-1829(98)07337-8]

I. INTRODUCTION

Amorphous carbon (*a*-C) materials have attracted considerable technological interest because they can be prepared with very high density and hardness.[1–3] In common with crystalline diamond, they also exhibit a high degree of transparency to the infrared and chemical inertness.[1,4] These properties have already led to applications for *a*-C as hard, wear-resistant coatings for mechanical and biological applications.[5,6] These materials also have the potential for application in the field of electronics: they have an optical band gap of over 2 eV, and can be *n*-type doped with both nitrogen and phosphorous.[7–9] *Ta*-C also has a low electron affinity which leads to applications as an electron emitter.

Tetrahedral amorphous carbon (*ta*-C) is a particular form of *a*-C which has a high proportion (>80%) of fourfold coordinated tetrahedral sp^3 sites. Experimental studies[10,11] have concluded that the structure of *ta*-C consists predominantly of a disordered tetrahedral network with a small contamination of sp^2 bonding and no discernible fraction of sp^1 bonds, but as yet, no model completely consistent with all the experimental data has been found.[12–21] *a*-C is difficult to model because of the variety of local bonding environments that the carbon atom can adopt. Many existing modeling techniques demand 100% fourfold coordination;[12,22,23] however, the interesting electronic properties of *ta*-C are completely determined by the distribution of sp^2 sites and their associated π bonds. It is therefore of crucial importance to establish a model for the atomic-scale structure which includes both sp^3 and sp^2 bonds. *Ab initio* models (e.g. Refs. 19–21) which generally produce realistic representations of the local bonding, are too small to provide statistical information on topological features such as clustering and ring-size distributions, and cannot reliably be compared with neutron diffraction data. Similarly, large empirical models such as that by Djordjevic *et al.*[24] do not treat local bonding correctly.

The reverse Monte Carlo[25] (RMC) technique can produce large three-dimensional models of the structure of disordered materials that agree quantitatively with the available experimental data, usually diffraction data. RMC is also a particularly appealing method because interatomic potentials, which are often difficult to define for amorphous networks but are essential to molecular dynamics and other Monte-Carlo based simulations, are not required. RMC has already been applied, with varying degrees of success, to modeling *a*-Si,[12] *a*-Ge,[12,26] and even *a*-C.[12,14]

However, in this work the detailed nature of the chemical bonding in amorphous carbon has been addressed explicitly.

II. RMC METHODS

The basic RMC algorithm has been described elsewhere.[25] In essence, "atoms" in a box are moved until the derived structure factor, $S_{\mathrm{mod}}(Q)$, and/or the associated pair correlation function, $g_{\mathrm{mod}}(r)$, matches the experimen-

tally measured data, $S_{expt}(Q)$ or $g_{expt}(r)$, where, for an amorphous material (i.e., an isotropic scatterer):[27]

$$S(Q)=1+\frac{4\pi\rho}{Q}\int_0^\infty r[g(r)-1]\sin(Qr)dr, \qquad (1)$$

where ρ is the number density of atoms in the material, $|\mathbf{Q}|=|\mathbf{k}_i-\mathbf{k}_f|$ is the wave vector transfer associated with the diffraction experiment and $g(r)$ is the pair distribution function, which is a measure of the atomic density at a distance r from a given atom at the origin. The pair distribution function may be obtained by Fourier transformation of the structure factor, which is directly related to the measured neutron scattering intensity. For each attempted move the quantity χ^2 is calculated, where $\chi^2=\Sigma_i[S_{expt}(Q_i)-S_{mod}(Q_i)]^2/\sigma_i$, and σ_i is the experimental error. The new configuration is accepted if the associated χ^2 has been reduced, and rejection is subject to a probability function dependent on the experimental error, σ_i. The process is repeated until $S_{mod}(Q)$ reproduces experiment, $S_{expt}(Q)$, to within the experimental errors. Where more than one data set, or any additional imposed constraints are used, the χ^2 calculations and the acceptance/rejection criteria, are applied to each.

For the models presented here a box edge of 27.14 Å was used, containing 3000 atoms placed initially at random sites (this corresponds to a density of 2.98 g cm^{-3}), subject to the criterion that the defined distances of closest approach were not violated. Using this box size implies that the significant oscillations in $g(r)$ should not extend beyond ~13.5 Å. This illustrates some of the important benefits of RMC: the large box size used in this study should significantly reduce truncation errors resulting from the finite model size, and allows the realistic generation of ensemble average figures for ring statistics, bond distances, coordination numbers, etc.

Neutron diffraction data was obtained by Gilkes *et al.*[14] in an experiment carried out at the ISIS pulsed neutron source (Rutherford Appleton Laboratory, UK), on the LAD diffractometer.[14] The Q-space experimental data were corrected for absorption and multiple and inelastic scattering using standard procedures.[28] Due to contamination of the sample with a small amount of crystalline graphite, scattering from powdered graphite measured under identical conditions was used to subtract the Bragg peaks, requiring truncation of the data at $Q=24.5$ Å.

$S(Q)$ and $g(r)$ were modeled simultaneously using a modified version of the original code supplied by McGreevy.[25] This was run on a DEC alpha 4000 processor, where on average ~10^7 moves may be attempted in a 24 hour period. The total number of accepted moves for the models present here was ~10^6. Considerations for deciding whether or not the model has reached equilibrium are generally based on the ratio of moves tried:moves accepted. The criterion we have adopted is that the algorithm be run until this ratio fell to ~1000:1, i.e., out of 1000 generated moves, only 1 move was found to be acceptable. During the fitting process, secondary minima were avoided by cycling the maximum displacement through the range 2 Å to 0.01 Å (and via the rejection probability function determined on the basis of the error, σ_i, associated with the experimental data).

A. Constraints for C bonding

In our work on amorphous hydrogenated carbon[29] (a-C:H) and amorphous germanium (a-Ge),[26] we have encountered several problems intrinsic to applying the RMC method to covalently bonded amorphous systems where diffraction data is used. This has led to the development of a number of constraints, which are applied to the model to avoid chemically and physically unreasonable features. This has been critical in trying to generate models of structures containing C-C bonds because of the variety of bond types that can be formed, i.e., sp^3, sp^2 or sp^1, and the associated range of first coordination numbers.

The models presented here differ in the type of constraints that have been applied and in the way that they have been defined. However, one common feature of all the models, is the definition of three different types of carbon atom. If we define a single bond by a near-neighbor distance, 1.40 Å $<r_s<$ 1.80 Å and a double bond by 1.28 Å$<r_d<$1.42 Å, then the three carbon atom types are as follows. Type 1 (C1): a C atom with four nearest neighbors at r_s, i.e., a tetrahedral sp^3 site; Type 2 (C2): a C atom with three nearest neighbors, two at r_s, and one r_d, i.e., a planar mixed sp^3-sp^2 site; and Type 3 (C3): a C atom with two nearest neighbors at r_d, i.e., a linear sp^2 site.

So, in accordance with the 84% sp^3 sites estimated directly from the experimental data[14] and the need to saturate double bonds, the 3000 atoms are distributed as follows; 2520 of type 1 (C1), 320 of type 2 (C2) and 160 of type 3 (C3). Note that it is assumed that the structure contains a negligible number of sp^1 C≡C bonds. This assumption is justified because there is no evidence in the experimental diffraction data that these bonds are present in significant numbers. A description of each model is now given.

B. Method I

In this method small units of 3, 4 or 5 atoms are defined by the coordination constraints and used to build a model of the network structure, referred to here as model A. This follows a similar philosophy to that of Ouyang and Ching[30] in their models of amorphous Si_3N_4. Considering only a central atom and its possible first neighbour atoms, there are 14 different configurations for these atom types, and these are shown in Fig. 1. Allowing all 14 was found to be far too computationally expensive to achieve a realistic model, so some configurations were selected as being more favorable than others. These chosen sites are (a), (b), (c), (f), (i), (j), (l) and (m), as shown in Fig. 1, with a ratio of 72:2:1:1:1:1:1:1 to maintain 84% sp^3 sites. In addition to these coordination constraints, a further constraint was applied to remove "triplets," i.e., three atoms forming an equilateral triangle with side length equal to a near-neighbor C-C distance. The existence of these is typified by a sharp peak in the bond angle distribution at 60° (Refs. 12,29) (and as revealed in model B, where this constraint was not used). The formation of these units results in three bonds at the required distance and therefore a relatively large fall in the χ^2 value, so they form very readily under the basic RMC algorithm. Such a conformation is highly strained and therefore may be considered as unlikely to occur in any substantial quantity. However, recent work by Marks *et al.*[13] using Car-Parrinello molecular dy-

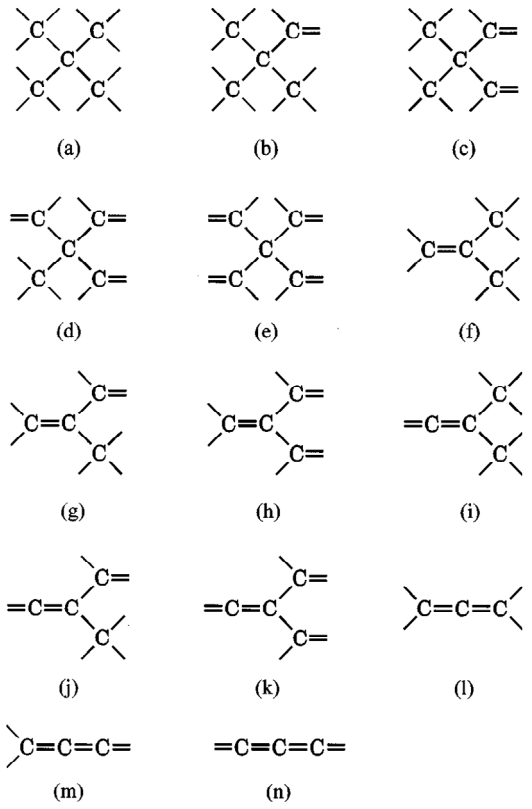

FIG. 1. The 14 possible bonding configurations, 8 of which [(a), (b), (c), (f), (i), (j), (l), and (m)] were used to produce model A.

namics to simulate the *ta*-C structure, argues *for* the possibility of both three- and four-membered rings, using evidence from organic chemistry to support their existence.

C. Method II

Two further models B and C have been produced using a completely new method of evaluating and applying coordination constraints.[31] This allows an sp^3 site to be defined as having four near-neighbors of type C1 or C2 and no near neighbors of type C3 at r_s. Similarly, a mixed sp^3-sp^2 site will have two near neighbors of type C1 or C2 at r_s and one near neighbor of type C2 or C3 at r_d and a planar sp^2 site will have two near neighbors of type C2 or C3 at r_d. In this way all of the configurations shown in Fig. 1 are possible with their probabilities determined by the ratio of atom types in the box. Since fewer coordination constraints are required in this method, the time taken to generate a satisfactory model is significantly reduced. This type of constraint also permits a more extensive exploration of configuration space.

The only difference between models B and C is that model C was also constrained to prevent the formation of 3-membered rings, as described above.

D. Method III

This method is similar to method II, but allows for the incorporation of hydrogen into the model, and was used to produce model D, containing 5 at. % H, i.e., 158 H atoms. Hydrogen has been included because there is a strong possibility that the sample used in the experiments has some hydrogen contamination (up to 5 at. %).[14] Whilst this may have a benign effect on the overall structure, the effect of network termination associated with hydrogen sites may prove to have been more significant, which may in turn have been reflected in the subtleties of $S(Q)$. In this method the C-H bond distance is defined as r_H, where $0.9\ \text{Å} < r_H < 1.28\ \text{Å}$. Therefore, C1 will have 4 nearest neighbors at r_s and/or r_H which will be of type C1, C2 or H; C2 will have 3 neighbors—1 of type C2 or C3 at r_d and 2 of type C1, C2 or H at r_s and/or r_H; and, as before, a C3 atom will have 2 neighbors at r_d of type C2 or C3. H is constrained to have 1 nearest neighbor at r_H, which can be either a C1 or C2 atom. The triplet constraint to remove three-membered rings was also applied to this model.

The properties and characteristics of each model are summarized in Table I.

III. RESULTS

A. Comparison with experimental data

Figure 2(a) shows the fits to the neutron diffraction $S(Q)$ for the four models. Beyond $\sim 6\ \text{Å}^{-1}$ the fits generated from the models are very similar, although they show a small displacement from the experimental data. This discrepancy probably results from the postulated small amount of hydrogen that will lead to some neutrons being scattered inelastically (and the data has not been corrected for this). In the region below $\sim 6\ \text{Å}^{-1}$ the models show much larger differences between each other and the experimental data. Model

TABLE I. A summary of the characteristics of the three different RMC models.

Model	Number of atoms				Density ($g\ cm^{-3}$)	Triplet constraint?	Type of coordination constraint	Fit to $S(Q)$?	Fit to $G(r)$?
	C1	C2	C3	H					
A	2520	320	160		2.98	Yes	Defined units of 3–5 atoms	Yes	Yes
B	2520	320	160		2.98	No	Allows a variety of near-neighbor types	Yes	Yes
C	2520	320	160		2.98	Yes	Allows a variety of near-neighbor types	Yes	Yes
D	2520	320	160	158	2.98	Yes	Allows a variety of near-neighbor types	Yes	Yes

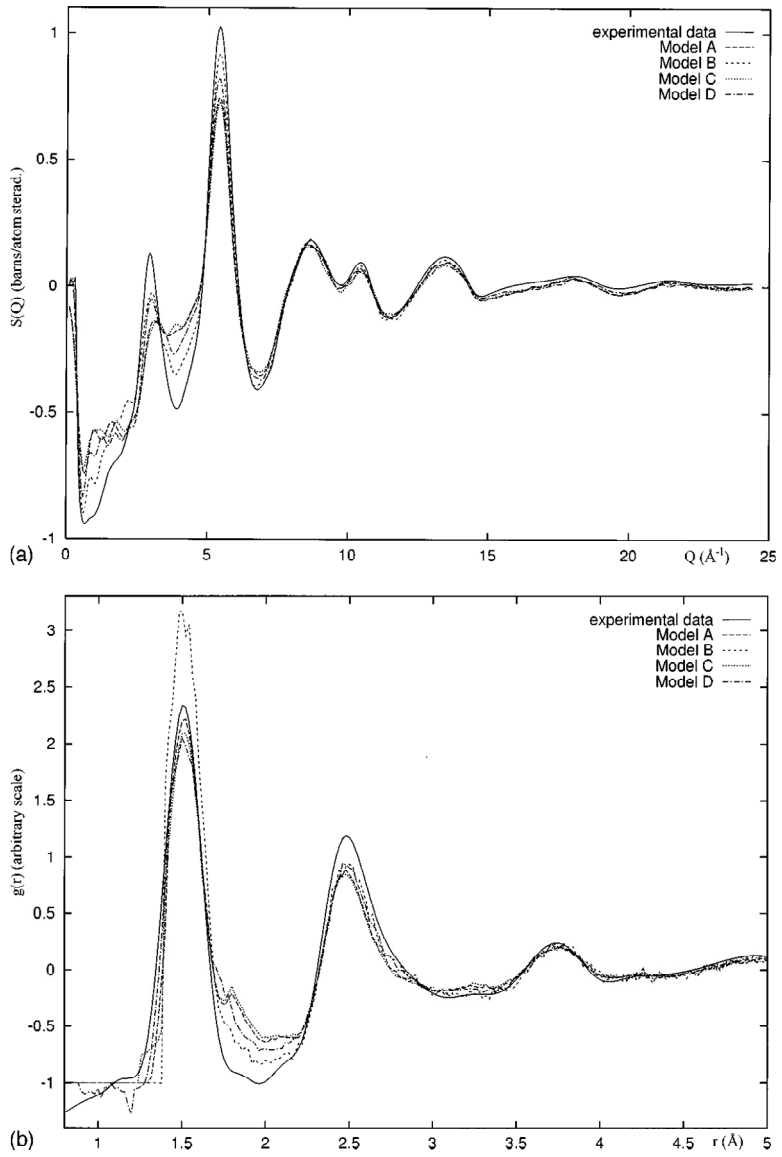

FIG. 2. (a) The fits to the experimental structure factor, $S(Q)$, generated from the four RMC models. (b) The fits to the experimental pair correlation function, $g(r)$, generated from the four RMC models. (c) The difference between the experimental structure factor, $S(Q)$, and the fits generated from the four RMC models (offset for clarity). (d) The difference between the experimental pair correlation function, $g(r)$, and the fits generated from the four RMC models (offset for clarity).

B, which has only coordination constraints and no triplet constraint, fits the data much more closely than the other models.

The real-space fits to $g(r)$ generated from our four models are shown in Fig. 2(b). Overall, the fits show good agreement with the experimental data, although there are some regions of discrepancy. The height of the first neighbor peak at ~1.5 Å is matched very well by models A and C, but model B has too high an intensity in this region.

Further, more detailed, information comparing the model-generated fits to the experimental data is provided by the difference plots presented in Figs. 2(c) and 2(d) for $S(Q)$ and $g(r)$, respectively.

B. Local bonding

Figure 3 shows the C bond angle distributions for all of the models. It is clear from these plots that a constraint to discourage three-membered rings with bond angles of 60° has not been applied to model B. The distribution for model A shows a broad peak centered around ~105° with additional peaks at ~70° and a small peak at ~60°. The peak at 60° is due to residual triplet configurations, while the peak at 70° probably results from the exclusion of 60° angles. The average bond angle for model A is found to be 106.7°.

The distribution for model B shows a similar peak at ~105°, which is less intense than that for model A, but also has a sharp peak at 60° due to the presence of triplets. This large intensity at 60° results in a lower average bond angle for this configuration of 102.6°. The bond angle distribution for model B is very similar to that observed in other RMC-generated models of various analogous systems.[12] The bond angle distribution for models C and D is similar to the distribution obtained for model A. At higher angles the distributions fall to zero smoothly, as observed for model B. The

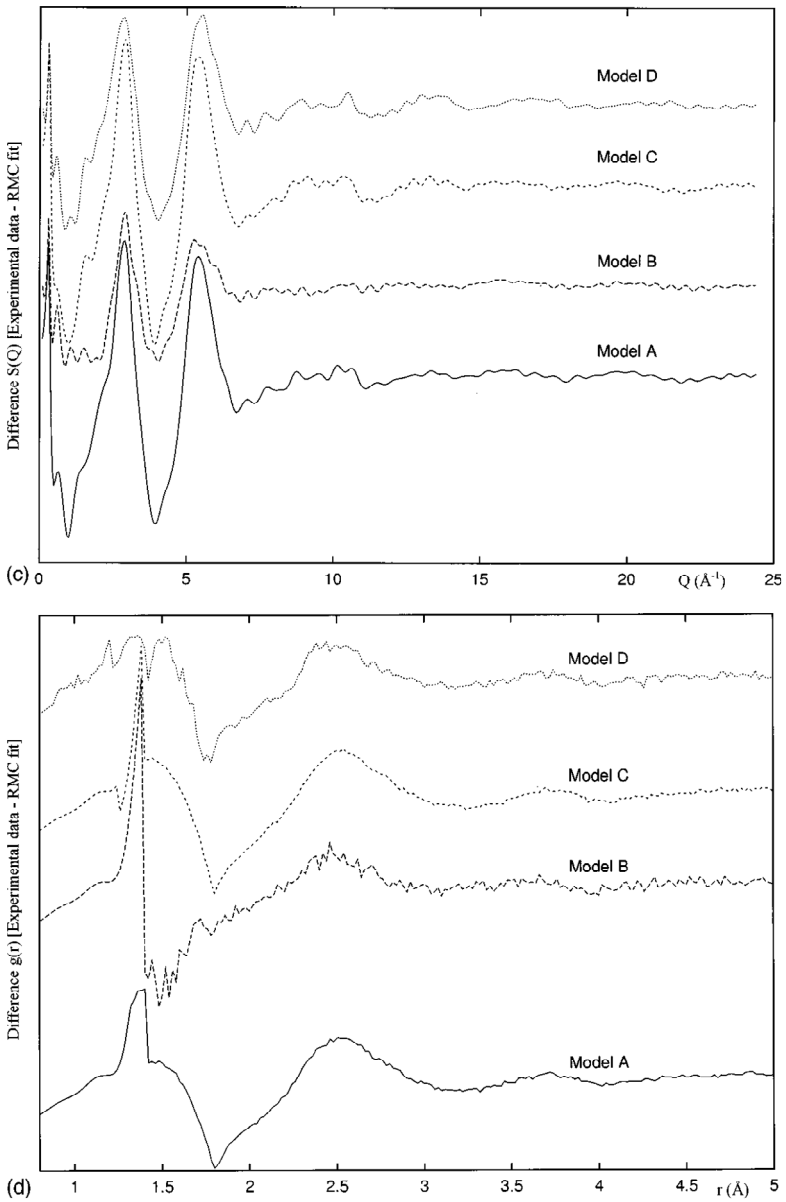

FIG. 2. (*Continued*).

average bond angle for model C is 109.0°, compared to 108.5° for model D. We can see that the addition of this small number of H atoms has little effect on the bond angle distribution of C atoms in the network. The average bond angles for these models are included in Table II, which also compares some of their other structural characteristics with those from a variety of models for *ta*-C.

Table III shows the average coordination numbers for the three C atom types in each of the models, together with the total average coordination numbers—these values are compared with those for other models in Table II. For all four models, over 94% of the C1 atom sites show the expected fourfold coordination and over 97% of C2 atoms are threefold coordinated. For the linear C3 bonding sites, 88% twofold coordination is achieved in model A, while the value is over 94% in models B, C, and D. This level of coordination is very satisfactory, considering the simplistic nature of the methods used to produce the networks, and these results show that the definition of three different types of carbon atom can be implemented successfully. The total average carbon coordination numbers are 3.74, 3.77, 3.72, and 3.59 for models A, B, C, and D, respectively. These values are all slightly lower than the experimentally determined figures, but are comparable to the values obtained in other simulation methods; see, for example, Refs. 14, 19, and 20. However, the average second coordination numbers from these four RMC models are significantly lower than the experimental value, and lower that for the other models in the table.

C. Topology

The ring size distributions calculated for the models are given in Table IV. In models A, C, and D the most favored number of atoms in a ring is 4, and for model B it is 3. Ignoring these smaller rings, we can see that for all the models except model B (including the WWW^{RMC} model[14]) the

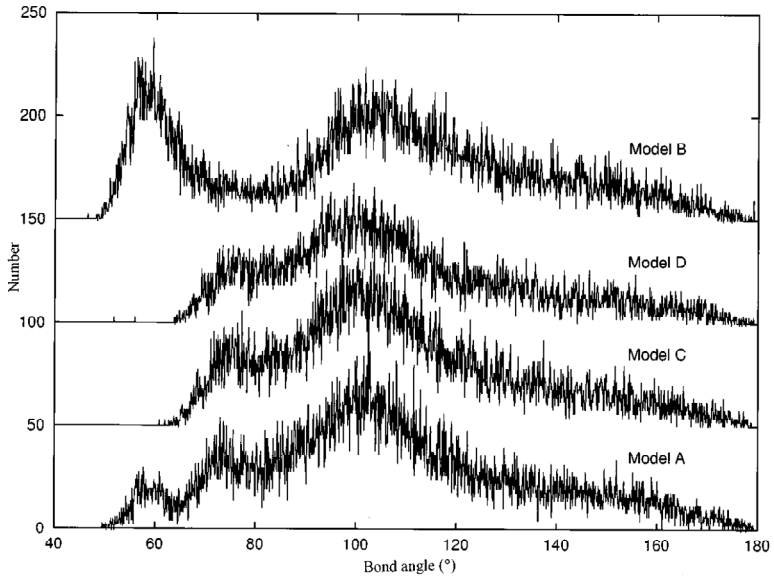

FIG. 3. Bond angle distributions obtained from the four model configurations (offset).

probability for different ring sizes is 5>6>7>8; although the difference between the number of five- and six-membered rings for these models is small. For model B the probability is 6>5>7>8.

Finally, Fig. 4 shows a 27 Å×27 Å×15 Å slice taken through the RMC box for model C. Figure 4(a) shows all the atom types, whereas Fig. 4(b) shows only C2 (blue) and C3 (yellow). Model C has been chosen to illustrate the results, but any of the three models could have been used, as the generic conclusions are the same.

IV. DISCUSSION

A. Comparison with experimental data

The nature of constraints and how they affect the fit to the experimental data can be understood very well by comparing the experimental $S(Q)$ and $g(r)$ functions with those obtained from the four RMC models. In particular, such a comparison yields valuable information as to the implications of defining short-range (i.e., nearest-neighbor) order on intermediate-range aspects of the structure. However, in the RMC method the experimental data itself acts as a constraint

TABLE II. Some characteristics of the models generated in this work compared to other models for *ta*-C. ($\langle\theta\rangle$ is the average bond angle and $\langle n_1\rangle$ and $\langle n_2\rangle$ are the average first and second coordination numbers.)

Model	Method	No. of atoms	Density (g cm^{-3})	sp^3 fraction	$\langle\theta\rangle$ (°)	r_1 (Å)	$\langle n_1\rangle$ (atoms)	r_2 (Å)	$\langle n_2\rangle$ (atoms)
Marks *et al.* (Ref. 13)	Car-Parrinello MD	64	2.9	65%		1.52	3.65	2.50	9.65
Djordjevic *et al.* (Ref. 24)	Wooten-Weaire	4096	1.583	100%	109.31	1.538	4		
Djordjevic *et al.* (Ref. 24)	Wooten-Weaire	4096	1.662	100%	109.30	1.513	4		
WWW^{RMC} Gilkes *et al.* (Ref. 14)	Wooten, Winer and Weaire+RMC	216	1.76	85%	109.65	1.53	3.85	2.45	11.06
Frauenheim *et al.* (Ref. 20)	Semiempirical MD	128	3.0	53%	112.0	1.51	3.53		
Drabold *et al.* (Ref. 19)	*Ab initio* MD	64	3.0	91%		1.566	3.91	2.583	10.69
Drabold *et al.* relaxed (Ref. 32)	*Ab initio* MD+DZP relaxation	64	3.0	72%		1.552	3.72	2.569	10.03
Model A	RMC	3000	2.98	84%	106.7	1.52	3.74	2.48	8.97
Model B	RMC	3000	2.98	84%	102.6	1.52	3.77	2.48	7.61
Model C	RMC	3000	2.98	84%	109.0	1.52	3.72	2.48	9.17
Model D	RMC	3158	2.98	84%	108.5	1.52	3.59	2.48	8.54
Experimental value			2.98	84%	109.3	1.52	3.84	2.48	11.31

TABLE III. The average coordination numbers for each of the atom types in the three models and the total average first coordination numbers.

Average coordination number	Model A	Model B	Model C	Model D	Physical value
C1	4.01	3.98	3.93	3.79	4.0
C2	2.50	2.67	2.43	2.91	3.0
C3	1.76	1.95	1.91	1.89	2.0
Total	3.74	3.77	3.72	3.59	

on the model, and it would be surprising therefore if a poor fit to the experimental data were obtained.

In general, the low-Q region (below ~ 6 Å^{-1}) of the structure factor is determined by the intermediate range order in the network, whereas features at higher Q-values arise from the short-range order, i.e., first nearest neighbors. Using RMC with coordination constraints automatically defines the required short-range order, but cannot control the order beyond the nearest neighbors in the model structure. Also, the triplet constraint gives some control over the first and second neighbors by ensuring that the bond angle formed by three connected atoms is not 60°, but has no other effect on the second neighbor atoms. Therefore, it is expected that the fit in the low-Q region will not be as good as for the high-Q region of the data. Indeed, this is clearly illustrated by the quality of the fit shown by each of the models [Figs. 2(a) and 2(c)]. Thus, model B (the least constrained) shows a better fit to the experimental Q-space data than model A (the most constrained). However, it is also noted that features in the low-Q region of the experimental data are the least reliable because they are most strongly affected by inelasticity in the neutron scattering. Problems in fitting Q-space data below ~ 4 Å^{-1} were also encountered by Frauenheim *et al.*[20] in their MD simulations of a-C materials. The fits to $S(Q)$ for models A–D are, however, better than that achieved by Djordjevic *et al.*[24] using the Wooten-Weaire method.

A better fit to the experimental diffraction data of Gaskell *et al.*[10] was achieved in the RMC models produced by Gereben and Pusztai,[12] but the fitting was done over a smaller Q-range and the models were less constrained. However, they also found that the imposition of *any* constraint resulted in a notable deterioration in the visual quality of the fit. It should be emphasised that a good fit to the experimental data does not automatically mean that a physically sensible model structure has been achieved. This point has been discussed recently for the case of vitreous silica by Keen,[32] where he states that "any valid structural model must be required to reproduce the experimental data, but it does not necessarily follow that the experimental data are sufficient to uniquely define a structural model." Hence, the quality of the fit to the data is not by itself a good measure of the quality of the structural model. It is also noted that many authors only calculate the real-space function, $g(r)$, from their models for comparison with the experimental data (Refs. 13, 14, 33, for example). In transforming from the experimental $S(Q)$ to $g(r)$, the clarity of the available information is always degraded due to truncation effects, therefore the nature of the agreement between the model $S(Q)$ and the experimental structure factor provides a better test of the model.

Consider now the fit to the real-space function, $g(r)$, generated by Fourier transform of $S(Q)$, as shown in Fig. 2(b). The height of the first neighbor peak at ~ 1.5 Å is matched very well by models A and C, but model B gives too much intensity in this region. This excess is almost certainly due to the absence of a triplets constraint in model B. In contrast, the small peak at ~ 1.8 Å is only observed in the models where the triplet constraint has been applied (A, C, and D) and is not seen in the experimental data. It is concluded that this peak arises from the bond-length limit used to define a triplet, and does not result from the distance limits for the coordination constraints. The triplet constraint requires an upper distance limit to define whether or not two atoms are bonded. Thus, the easiest way to remove atoms involved in 3-membered rings inside this distance, and thereby to satisfy the triplet constraint, is to move them just outside this distance limit. This leads to a build up of atoms at ~ 1.8 Å, as seen in the models which include the triplet constraint. Note that a small peak at this distance was also observed in two of the RMC models by Gereben and Pusztai[12] where the coordination constraints demanded over 90% fourfold coordination. Therefore, this peak would appear to be a characteristic of an over-constrained network.

It is interesting that the fits to $g(r)$ from all four models show a lower intensity in the second neighbor peak (~ 2.5 Å)

TABLE IV. Ring statistics for the four new models compared to two other models for ta-C. The values for the number of rings for each size are the number of rings per site.

Ring size	3	4	5	6	7	8
Model A	0.11	0.37	0.20	0.19	0.11	0.05
Model B	0.43	0.18	0.13	0.18	0.09	0.07
Model C	0	0.33	0.23	0.18	0.12	0.06
Model D	0	0.26	0.16	0.13	0.07	0.04
WWW^{RMC} (Ref. 14)	0	0.03	0.39	0.38	0.12	0
Marks *et al.* (Ref. 13)	0.05	0.05	0.33	0.30	0.14	0.17

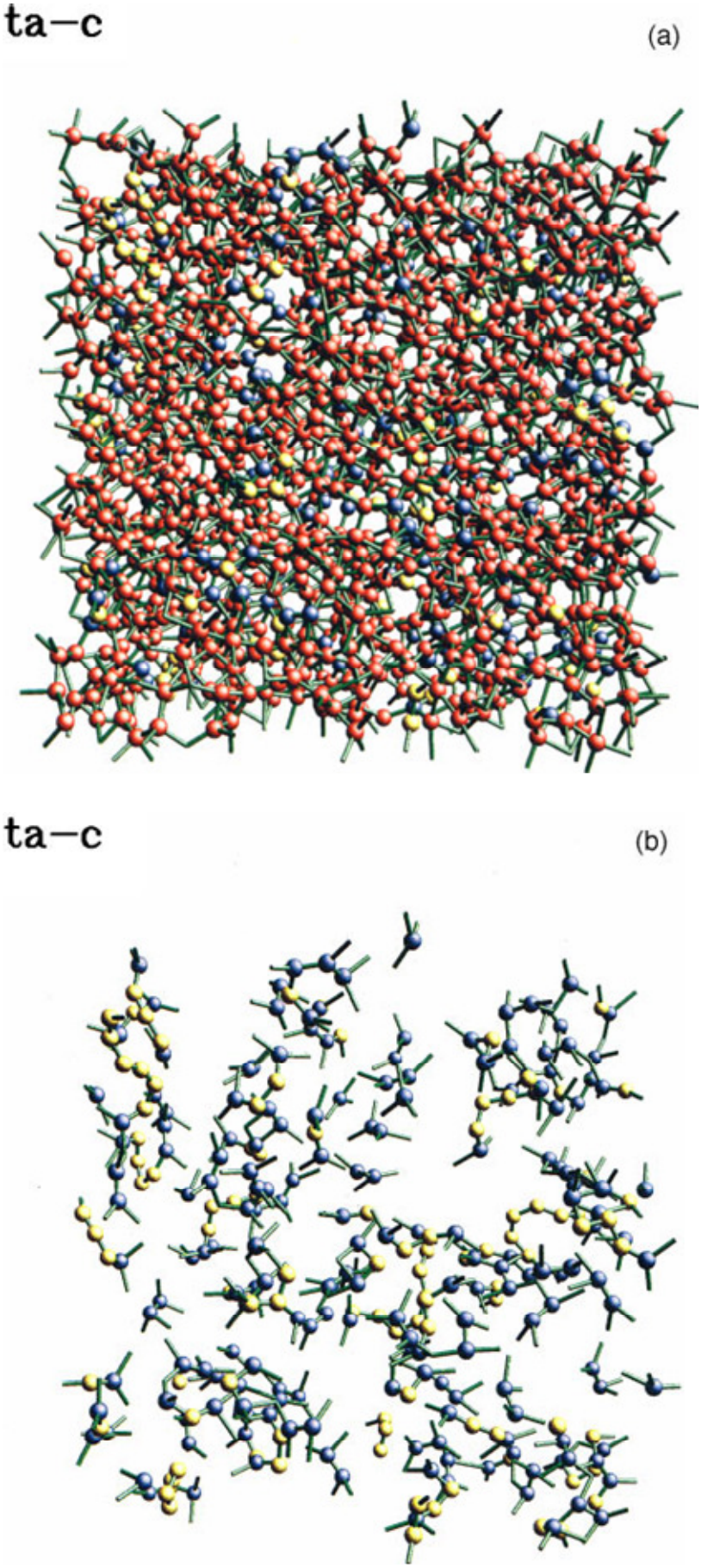

FIG. 4. (Color) (a) A slice taken through the configuration for model C, showing the distribution of the three different types of carbon atom: C1 (red), C2 (blue), and C3 (yellow). (b) A slice taken through the configuration for model C, showing the C2 (blue) and C3 (yellow) carbon atoms in chains and small clusters.

and a greater intensity between the first and second neighbor peaks, compared to the experimental data. Once again, this is evidence of the difficulty in reproducing intermediate-range order using this method, probably because the short-range order is so well defined by the imposition of coordination and triplet constraints. By the third neighbor peak (~3.8 Å) the structure is so disordered that this effect can no longer be seen.

B. Local bonding and network topology

The bond angle distributions for the four models (Fig. 3) show clearly the effects of using the triplet constraint to remove three-membered rings. In the description of method I, the need to use the triplet constraint on models produced by the RMC algorithm was explained, and this can be justified if the bond angle distributions for models B and C, for example, are compared—the sharp peak at 60° characteristic of a structure containing a large number of three-membered rings is obvious in the distribution for model B. This has been observed in other models,[12,29] and is a fundamental problem in the application of RMC to modeling this type of material.

In general, the exclusion of 60° bond angles results in an increase in the intensity on the low angle side of the main peak in the distribution (~105°). This is because many of the atomic positions that would have given 60° angles are forced to adopt configurations with higher bond angles. It appears that the easiest way to fit this with the experimental data is to produce bond angles between ~65 and ~90°. This effect can be seen in the bond angle distributions for models C and D, and to a lesser extent for model A.

Also, for model A, instead of decaying smoothly to zero, the distribution at high angle has a very broad peak, which is unique to this model. It is not possible to assign it to a particular bonding configuration; however, it may well result from the nature of the constraints used in this model. Model A is more tightly constrained at the first neighbor level than the others, and this probably results in some unusual and highly strained configurations of atoms, which produce additional bond angles in this high angle range of the distribution.

The constraint to exclude three-membered rings also has a marked effect on the ring statistics (see Table IV). It is immediately obvious from Table IV that where 3-membered rings are permitted, i.e., in model B, there are an enormous number of them in the structure. Whereas in the models where the triplet constraint has been applied (A, C, and D), this results in a dramatic increase in the number of four-membered rings. There has been some recent discussion in the literature[13,33] about whether or not such small rings can occur, or indeed are necessary to achieve a good model for the structure of *ta*-C. For example, the simulated structures of Drabold *et al.*[19] and Marks *et al.*[13] both contain a small but significant number of three- and four-membered rings. Schultze and Stechel[33] go so far as to say that their existence in the simulations provides good evidence that they are present in *ta*-C. However, no other simulation method leads to as many small rings as are formed in our RMC structures and it is therefore important to recall that the presence of large numbers of them has more to do with the way in which the RMC algorithm works, and the manner in which it is applied, than to physical reality. They are, in other words, anticipated artifacts of the method.

Some evidence of the more subtle effects of constraining the models can also be found upon examination of the coordination information (Tables II and III). Model B, which does not have the additional triplet constraint and therefore has more freedom than the other models, has the highest average coordination number. However, it is interesting to note that, in terms of the coordination numbers at least, models A and C, which were generated by quite different methods, appear to be equally successful. There is also some evidence, from the slightly lower average coordination number in model D, of the network terminating effect of H. The inability of these models to generate sufficiently high average second coordination numbers is another sign of the relatively poor reproduction of intermediate-range order in the structure.

Recent models obtained by Schultze and Stechel[33] from relaxing models for *ta*-C obtained by other authors[13,17,19,34] have explored the distribution of threefold coordinated atoms within their model structures. They found that threefold coordinated atoms appear mostly in pairs or in even-numbered clusters, and that although the threefold coordinated atoms coalesce, there is no sign of aromatic ring structures. However, it should be noted that the largest model they use consists of only 216 atoms and that they have no twofold coordinated atoms. We can look at the same distributions for our models, which consist of 3000 atoms, and slices taken through the simulation box are shown in Figs. 4(a) and 4(b). Figure 4(a) shows that we have generated a disordered tetrahedral network, which contains both highly dense areas of C1 atoms, and less dense areas which tend to be bordered by C2 and C3 atoms. This is consistent with the "diamond-like" properties of the material, where the high hardness results from the disordered tetrahedral regions of C1 atoms, and the strong cross-linking of these by polymerlike chains and small clusters containing sp^2 bonds. The existence of these chains and small clusters can be clearly seen in Fig. 4(b). Also, Fig. 4(b) shows that the sp^2 bonds do not form graphitic/aromatic rings, but act like a polymeric "glue" holding the sp^3 regions together. This is in qualitative agreement with the results of Schultze and Stechel,[33] although for our models an examination of the clustering is arguably more meaningful because of the box size.

V. CONCLUSIONS

It is clear from the discussion of the four models presented here that the RMC method has both advantages and disadvantages. The question now is how one can best exploit its advantages. A large box-size is necessary for looking at properties of the model that involve atoms beyond the nearest-neighbors (e.g., clustering of atom types, ring sizes, etc.), however, before this can be useful one needs to be able to generate a reasonable model structure. It is becoming increasingly apparent with the development of more sophisticated molecular dynamics simulation methods that the energy of the network structure needs to be considered. This is not done in the RMC method. However, RMC does offer the chance to build a model structure which is consistent with experimental diffraction data and which obeys a set of rules

for local bonding. Further, the present results show that by defining near-neighbor atom types and bond distances, the correct chemical bonding can be built up relatively easily.

We have seen that introducing constraints on the local bonding leads to problems achieving the required intermediate-range order, i.e., beyond the nearest neighbors. It is possible that, by a similar method, constraints on the type and distances of second neighbors could also be developed, but defining a set of rules for this would be very difficult. There would also be a dramatic increase in the number of constraints, making it computationally costly to obtain a model satisfying them all. The problems with the three- and four-membered rings could also be remedied by fitting to a ring-size distribution. But, the distribution to be fitted would always involve *a-priori* bias as it cannot be obtained directly from the experimental data (and this would again slow down the algorithm considerably). Both cases would require additional information to be fed into the RMC method, which means that the ability to explore configuration-space widely in a controlled way, and thereby to try to generate fresh insights into the attributes of the network structure, becomes even smaller.

For these reasons it is suggested that the future application of the RMC method to modeling amorphous carbon, and other comparable systems, will be in generating a model which may then be used as the starting configuration for more sophisticated simulation methods. This would, for instance, by-pass a time-consuming stage in *ab initio* methods where the correct chemical bonding has to be reached, and would mean that larger simulation cells could be used. The RMC configuration has the added advantage that the structure is consistent with experimental data from the start. We are already investigating this application by relaxing the configuration of model C with a tight-binding method, for subsequent input into an MD simulation.

ACKNOWLEDGMENTS

J.K.W. is grateful to the Royal 1851 Commission for their generous financial support. We are grateful to P. Schultze and E. Stechel for providing a copy of their paper in advance of its publication and to G. Galli and F. Mauri for stimulating discussions regarding the potential use for the RMC models within simulation methods.

[1] J. Robertson, Prog. Solid State Chem. **21**, 199 (1991); Philos. Trans. R. Soc. London, Ser. A **342**, 277 (1993).
[2] D. R. McKenzie, D. Muller, and B. A. Pailthorpe, Phys. Rev. Lett. **67**, 773 (1991).
[3] Y. Lifshitz, S. R. Kasi, and J. W. Rabalais, Phys. Rev. Lett. **68**, 628 (1989).
[4] R. Lossy, D. L. Pappas, R. A. Roy, and J. J. Cuomo, Appl. Phys. Lett. **61**, 171 (1989).
[5] A. H. Lettington, in *Diamond and Diamondlike Films and Coatings*, edited by J. C. Angus, R. E. Clausing, L. L. Horton, and P. Koidl (Plenum, New York, 1991).
[6] S. Aisenberg and F. M. Kimock, Mater. Sci. Forum **52–53**, 1 (1989).
[7] V. S. Veerasamy, G. A. J. Amaratunga, C. A. Davis, W. I. Milne, P. Hewitt, and M. Weiler, Solid-State Electron. **37**, 319 (1994).
[8] V. S. Veerasamy, J. Yuan, G. A. J. Amaratunga, W. I. Milne, K. W. R. Gilkes, M. Weiler, and L. M. Brown, Phys. Rev. B **48**, 17 954 (1993).
[9] V. S. Veerasamy, G. A. J. Amaratunga, C. A. Davis, A. E. Timbs, W. I. Milne, and D. R. McKenzie, J. Phys.: Condens. Matter **5**, L169 (1993).
[10] P. H. Gaskell, A. Saeed, P. Chieux, and D. R. McKenzie, Phys. Rev. Lett. **67**, 1286 (1991).
[11] S. D. Berger, D. R. McKenzie, and P. J. Martin, Philos. Mag. Lett. **57**, 6 (1988).
[12] O. Gereben and L. Pusztai, Phys. Rev. B **50**, 14 136 (1994).
[13] N. A. Marks, D. R. McKenzie, B. A. Pailthorpe, M. Bernasconi, and M. Parrinello, Phys. Rev. B **54**, 9703 (1996).
[14] K. W. R. Gilkes, P. H. Gaskell, and J. Robertson, Phys. Rev. B **51**, 12 303 (1995).
[15] J. Tersoff, Phys. Rev. Lett. **61**, 2879 (1988).
[16] P. C. Kelires, Phys. Rev. Lett. **68**, 1854 (1992).
[17] C. Z. Wang, K. M. Ho, and C. T. Chan, Phys. Rev. Lett. **71**, 1184 (1993).
[18] U. Stephan, Th. Frauenheim, P. Blaudeck, and G. Jungnickel, Phys. Rev. B **49**, 1489 (1994).
[19] D. A. Drabold, P. A. Fedders, and P. Stumm, Phys. Rev. B **49**, 16 415 (1994).
[20] Th. Frauenheim, P. Blaudeck, U. Stephan, and G. Jungnickel, Phys. Rev. B **48**, 4823 (1993).
[21] G. Galli, R. Martin, R. Car, and M. Parrinello, Phys. Rev. Lett. **62**, 555 (1989); Phys. Rev. B **42**, 7470 (1990).
[22] F. Wooten and D. Weaire, J. Non-Cryst. Solids **64**, 325 (1984); F. Wooten, K. Winer, and D. Weaire, Phys. Rev. Lett. **54**, 1392 (1985).
[23] D. E. Polk and D. S. Boudreaux, Phys. Rev. Lett. **31**, 92 (1973).
[24] B. R. Djordjevic, M. F. Thorpe, and F. Wooten, Phys. Rev. B **52**, 5685 (1995).
[25] R. L. McGreevy and L. Pusztai, Mol. Simul. **1**, 359 (1988).
[26] J. K. Walters and R. J. Newport, Phys. Rev. B **53**, 2405 (1996).
[27] R. J. Newport, in *Neutron Scattering at a Pulsed Source*, edited by R. J. Newport, B. D. Rainford, and R. Cywinski (Hilger, Bristol, 1988), Chap. 13, p. 233; N. E. Cusack, *The Physics of Structurally Disordered Matter* (Hilger, Bristol, 1987).
[28] M. A. Howe, R. L. McGreevy, and W. S. Howells, J. Phys.: Condens. Matter **1**, 3433 (1989).
[29] J. K. Walters, J. S. Rigden, and R. J. Newport, Phys. Scr. **T57**, 137 (1995).
[30] L. Ouyang and W. Y. Ching, Phys. Rev. B **54**, 15 594 (1996).
[31] J. K. Walters, K. W. R. Gilkes, J. D. Wicks, and R. J. Newport, J. Phys.: Condens. Matter **9**, L457 (1997).
[32] D. A. Keen, Phase Transit. **61**, 109 (1997).
[33] P. A. Schultz and E. B. Stechel, Phys. Rev. B **57**, 3295 (1998).
[34] C. Z. Wang and K. M. Ho, Phys. Rev. B **50**, 12 429 (1994).